10-4-2011

Search for Lepton-Number Violating Processes in B+ -> h- l+ l+ Decays

Raymond Mountain
Syracuse University

Marina Artuso
Department of Physics, Syracuse University, Syracuse, NY

S. Blusk
Syracuse University

Alessandra Borgia
Syracuse University

EUROPEAN ORGANIZATION FOR NUCLEAR RESEARCH (CERN)

LHCb-PAPER-2011-009
CERN-PH-EP-2011-156
October 5, 2011

Search for the lepton number violating decays $B^+ \to \pi^- \mu^+ \mu^+$ and $B^+ \to K^- \mu^+ \mu^+$

R. Aaij[23], C. Abellan Beteta[35,n], B. Adeva[36], M. Adinolfi[42], C. Adrover[6], A. Affolder[48], Z. Ajaltouni[5], J. Albrecht[37], F. Alessio[37], M. Alexander[47], G. Alkhazov[29], P. Alvarez Cartelle[36], A.A. Alves Jr[22], S. Amato[2], Y. Amhis[38], J. Anderson[39], R.B. Appleby[50], O. Aquines Gutierrez[10], F. Archilli[18,37], L. Arrabito[53], A. Artamonov [34], M. Artuso[52,37], E. Aslanides[6], G. Auriemma[22,m], S. Bachmann[11], J.J. Back[44], D.S. Bailey[50], V. Balagura[30,37], W. Baldini[16], R.J. Barlow[50], C. Barschel[37], S. Barsuk[7], W. Barter[43], A. Bates[47], C. Bauer[10], Th. Bauer[23], A. Bay[38], I. Bediaga[1], K. Belous[34], I. Belyaev[30,37], E. Ben-Haim[8], M. Benayoun[8], G. Bencivenni[18], S. Benson[46], J. Benton[42], R. Bernet[39], M.-O. Bettler[17], M. van Beuzekom[23], A. Bien[11], S. Bifani[12], A. Bizzeti[17,h], P.M. Bjørnstad[50], T. Blake[49], F. Blanc[38], C. Blanks[49], J. Blouw[11], S. Blusk[52], A. Bobrov[33], V. Bocci[22], A. Bondar[33], N. Bondar[29], W. Bonivento[15], S. Borghi[47], A. Borgia[52], T.J.V. Bowcock[48], C. Bozzi[16], T. Brambach[9], J. van den Brand[24], J. Bressieux[38], D. Brett[50], S. Brisbane[51], M. Britsch[10], T. Britton[52], N.H. Brook[42], H. Brown[48], A. Büchler-Germann[39], I. Burducea[28], A. Bursche[39], J. Buytaert[37], S. Cadeddu[15], J.M. Caicedo Carvajal[37], O. Callot[7], M. Calvi[20,j], M. Calvo Gomez[35,n], A. Camboni[35], P. Campana[18,37], A. Carbone[14], G. Carboni[21,k], R. Cardinale[19,i,37], A. Cardini[15], L. Carson[36], K. Carvalho Akiba[23], G. Casse[48], M. Cattaneo[37], M. Charles[51], Ph. Charpentier[37], N. Chiapolini[39], K. Ciba[37], X. Cid Vidal[36], G. Ciezarek[49], P.E.L. Clarke[46,37], M. Clemencic[37], H.V. Cliff[43], J. Closier[37], C. Coca[28], V. Coco[23], J. Cogan[6], P. Collins[37], A. Comerma-Montells[35], F. Constantin[28], G. Conti[38], A. Contu[51], A. Cook[42], M. Coombes[42], G. Corti[37], G.A. Cowan[38], R. Currie[46], B. D'Almagne[7], C. D'Ambrosio[37], P. David[8], I. De Bonis[4], S. De Capua[21,k], M. De Cian[39], F. De Lorenzi[12], J.M. De Miranda[1], L. De Paula[2], P. De Simone[18], D. Decamp[4], M. Deckenhoff[9], H. Degaudenzi[38,37], M. Deissenroth[11], L. Del Buono[8], C. Deplano[15], O. Deschamps[5], F. Dettori[15,d], J. Dickens[43], H. Dijkstra[37], P. Diniz Batista[1], F. Domingo Bonal[35,n], S. Donleavy[48], A. Dosil Suárez[36], D. Dossett[44], A. Dovbnya[40], F. Dupertuis[38], R. Dzhelyadin[34], S. Easo[45], U. Egede[49], V. Egorychev[30], S. Eidelman[33], D. van Eijk[23], F. Eisele[11], S. Eisenhardt[46], R. Ekelhof[9], L. Eklund[47], Ch. Elsasser[39], D.G. d'Enterria[35,o], D. Esperante Pereira[36], L. Estève[43], A. Falabella[16,e], E. Fanchini[20,j], C. Färber[11], G. Fardell[46], C. Farinelli[23], S. Farry[12], V. Fave[38], V. Fernandez Albor[36], M. Ferro-Luzzi[37], S. Filippov[32], C. Fitzpatrick[46], M. Fontana[10], F. Fontanelli[19,i], R. Forty[37], M. Frank[37], C. Frei[37], M. Frosini[17,f,37], S. Furcas[20], A. Gallas Torreira[36], D. Galli[14,c], M. Gandelman[2], P. Gandini[51], Y. Gao[3], J-C. Garnier[37], J. Garofoli[52], J. Garra Tico[43], L. Garrido[35], D. Gascon[35], C. Gaspar[37], N. Gauvin[38], M. Gersabeck[37], T. Gershon[44,37], Ph. Ghez[4], V. Gibson[43], V.V. Gligorov[37], C. Göbel[54], D. Golubkov[30], A. Golutvin[49,30,37], A. Gomes[2], H. Gordon[51], M. Grabalosa Gándara[35], R. Graciani Diaz[35], L.A. Granado Cardoso[37], E. Graugés[35], G. Graziani[17], A. Grecu[28], E. Greening[51], S. Gregson[43], B. Gui[52], E. Gushchin[32], Yu. Guz[34], T. Gys[37], G. Haefeli[38], C. Haen[37], S.C. Haines[43], T. Hampson[42], S. Hansmann-Menzemer[11], R. Harji[49], N. Harnew[51], J. Harrison[50], P.F. Harrison[44], J. He[7], V. Heijne[23], K. Hennessy[48], P. Henrard[5], J.A. Hernando Morata[36], E. van Herwijnen[37], E. Hicks[48], W. Hofmann[10], K. Holubyev[11], P. Hopchev[4], W. Hulsbergen[23], P. Hunt[51], T. Huse[48], R.S. Huston[12], D. Hutchcroft[48], D. Hynds[47], V. Iakovenko[41], P. Ilten[12], J. Imong[42], R. Jacobsson[37], A. Jaeger[11], M. Jahjah Hussein[5], E. Jans[23], F. Jansen[23], P. Jaton[38], B. Jean-Marie[7], F. Jing[3], M. John[51], D. Johnson[51], C.R. Jones[43], B. Jost[37], S. Kandybei[40], M. Karacson[37], T.M. Karbach[9], J. Keaveney[12], U. Kerzel[37], T. Ketel[24], A. Keune[38], B. Khanji[6], Y.M. Kim[46], M. Knecht[38], S. Koblitz[37], P. Koppenburg[23], A. Kozlinskiy[23], L. Kravchuk[32], K. Kreplin[11], M. Kreps[44], G. Krocker[11], P. Krokovny[11], F. Kruse[9], K. Kruzelecki[37], M. Kucharczyk[20,25,37], S. Kukulak[25], R. Kumar[14,37], T. Kvaratskheliya[30,37], V.N. La Thi[38], D. Lacarrere[37], G. Lafferty[50], A. Lai[15], D. Lambert[46], R.W. Lambert[37], E. Lanciotti[37], G. Lanfranchi[18], C. Langenbruch[11], T. Latham[44], R. Le Gac[6], J. van Leerdam[23], J.-P. Lees[4], R. Lefèvre[5], A. Leflat[31,37], J. Lefrançois[7], O. Leroy[6], T. Lesiak[25], L. Li[3], L. Li Gioi[5], M. Lieng[9], M. Liles[48], R. Lindner[37], C. Linn[11], B. Liu[3], G. Liu[37], J.H. Lopes[2], E. Lopez Asamar[35], N. Lopez-March[38], J. Luisier[38], F. Machefert[7], I.V. Machikhiliyan[4,30], F. Maciuc[10], O. Maev[29,37], J. Magnin[1], S. Malde[51], R.M.D. Mamunur[37],

G. Manca[15,d], G. Mancinelli[6], N. Mangiafave[43], U. Marconi[14], R. Märki[38], J. Marks[11], G. Martellotti[22], A. Martens[7], L. Martin[51], A. Martín Sánchez[7], D. Martinez Santos[37], A. Massafferri[1], Z. Mathe[12], C. Matteuzzi[20], M. Matveev[29], E. Maurice[6], B. Maynard[52], A. Mazurov[16,32,37], G. McGregor[50], R. McNulty[12], C. Mclean[14], M. Meissner[11], M. Merk[23], J. Merkel[9], R. Messi[21,k], S. Miglioranzi[37], D.A. Milanes[13,37], M.-N. Minard[4], S. Monteil[5], D. Moran[12], P. Morawski[25], R. Mountain[52], I. Mous[23], F. Muheim[46], K. Müller[39], R. Muresan[28,38], B. Muryn[26], M. Musy[35], J. Mylroie-Smith[48], P. Naik[42], T. Nakada[38], R. Nandakumar[45], J. Nardulli[45], I. Nasteva[1], M. Nedos[9], M. Needham[46], N. Neufeld[37], C. Nguyen-Mau[38,p], M. Nicol[7], S. Nies[9], V. Niess[5], N. Nikitin[31], A. Nomerotski[51], A. Oblakowska-Mucha[26], V. Obraztsov[34], S. Oggero[23], S. Ogilvy[47], O. Okhrimenko[41], R. Oldeman[15,d], M. Orlandea[28], J.M. Otalora Goicochea[2], P. Owen[49], K. Pal[52], J. Palacios[39], A. Palano[13,b], M. Palutan[18], J. Panman[37], A. Papanestis[45], M. Pappagallo[13,b], C. Parkes[47,37], C.J. Parkinson[49], G. Passaleva[17], G.D. Patel[48], M. Patel[49], S.K. Paterson[49], G.N. Patrick[45], C. Patrignani[19,i], C. Pavel-Nicorescu[28], A. Pazos Alvarez[36], A. Pellegrino[23], G. Penso[22,l], M. Pepe Altarelli[37], S. Perazzini[14,c], D.L. Perego[20,j], E. Perez Trigo[36], A. Pérez-Calero Yzquierdo[35], P. Perret[5], M. Perrin-Terrin[6], G. Pessina[20], A. Petrella[16,37], A. Petrolini[19,i], E. Picatoste Olloqui[35], B. Pie Valls[35], B. Pietrzyk[4], T. Pilar[44], D. Pinci[22], R. Plackett[47], S. Playfer[46], M. Plo Casasus[36], G. Polok[25], A. Poluektov[44,33], E. Polycarpo[2], D. Popov[10], B. Popovici[28], C. Potterat[35], A. Powell[51], T. du Pree[23], J. Prisciandaro[38], V. Pugatch[41], A. Puig Navarro[35], W. Qian[52], J.H. Rademacker[42], B. Rakotomiaramanana[38], M.S. Rangel[2], I. Raniuk[40], G. Raven[24], S. Redford[51], M.M. Reid[44], A.C. dos Reis[1], S. Ricciardi[45], K. Rinnert[48], D.A. Roa Romero[5], P. Robbe[7], E. Rodrigues[47], F. Rodrigues[2], P. Rodriguez Perez[36], G.J. Rogers[43], S. Roiser[37], V. Romanovsky[34], M. Rosello[35,n], J. Rouvinet[38], T. Ruf[37], H. Ruiz[35], G. Sabatino[21,k], J.J. Saborido Silva[36], N. Sagidova[29], P. Sail[47], B. Saitta[15,d], C. Salzmann[39], M. Sannino[19,i], R. Santacesaria[22], R. Santinelli[37], E. Santovetti[21,k], M. Sapunov[6], A. Sarti[18,l], C. Satriano[22,m], A. Satta[21], M. Savrie[16,e], D. Savrina[30], P. Schaack[49], M. Schiller[11], S. Schleich[9], M. Schmelling[10], B. Schmidt[37], O. Schneider[38], A. Schopper[37], M.-H. Schune[7], R. Schwemmer[37], B. Sciascia[18], A. Sciubba[18,l], M. Seco[36], A. Semennikov[30], K. Senderowska[26], I. Sepp[49], N. Serra[39], J. Serrano[6], P. Seyfert[11], B. Shao[3], M. Shapkin[34], I. Shapoval[40,37], P. Shatalov[30], Y. Shcheglov[29], T. Shears[48], L. Shekhtman[33], O. Shevchenko[40], V. Shevchenko[30], A. Shires[49], R. Silva Coutinho[54], H.P. Skottowe[43], T. Skwarnicki[52], A.C. Smith[37], N.A. Smith[48], E. Smith[51,45], K. Sobczak[5], F.J.P. Soler[47], A. Solomin[42], F. Soomro[49], B. Souza De Paula[2], B. Spaan[9], A. Sparkes[46], P. Spradlin[47], F. Stagni[37], S. Stahl[11], O. Steinkamp[39], S. Stoica[28], S. Stone[52,37], B. Storaci[23], M. Straticiuc[28], U. Straumann[39], N. Styles[46], V.K. Subbiah[37], S. Swientek[9], M. Szczekowski[27], P. Szczypka[38], T. Szumlak[26], S. T'Jampens[4], E. Teodorescu[28], F. Teubert[37], C. Thomas[51,45], E. Thomas[37], J. van Tilburg[11], V. Tisserand[4], M. Tobin[39], S. Topp-Joergensen[51], N. Torr[51], M.T. Tran[38], A. Tsaregorodtsev[6], N. Tuning[23], A. Ukleja[27], P. Urquijo[52], U. Uwer[11], V. Vagnoni[14], G. Valenti[14], R. Vazquez Gomez[35], P. Vazquez Regueiro[36], S. Vecchi[16], J.J. Velthuis[42], M. Veltri[17,g], K. Vervink[37], B. Viaud[7], I. Videau[7], X. Vilasis-Cardona[35,n], J. Visniakov[36], A. Vollhardt[39], D. Voong[42], A. Vorobyev[29], H. Voss[10], K. Wacker[9], S. Wandernoth[11], J. Wang[52], D.R. Ward[43], A.D. Webber[50], D. Websdale[49], M. Whitehead[44], D. Wiedner[11], L. Wiggers[23], G. Wilkinson[51], M.P. Williams[44,45], M. Williams[49], F.F. Wilson[45], J. Wishahi[9], M. Witek[25], W. Witzeling[37], S.A. Wotton[43], K. Wyllie[37], Y. Xie[46], F. Xing[51], Z. Xing[52], Z. Yang[3], R. Young[46], O. Yushchenko[34], M. Zavertyaev[10,a], L. Zhang[52], W.C. Zhang[12], Y. Zhang[3], A. Zhelezov[11], L. Zhong[3], E. Zverev[31], A. Zvyagin [37].

[1] *Centro Brasileiro de Pesquisas Físicas (CBPF), Rio de Janeiro, Brazil*
[2] *Universidade Federal do Rio de Janeiro (UFRJ), Rio de Janeiro, Brazil*
[3] *Center for High Energy Physics, Tsinghua University, Beijing, China*
[4] *LAPP, Université de Savoie, CNRS/IN2P3, Annecy-Le-Vieux, France*
[5] *Clermont Université, Université Blaise Pascal, CNRS/IN2P3, LPC, Clermont-Ferrand, France*
[6] *CPPM, Aix-Marseille Université, CNRS/IN2P3, Marseille, France*
[7] *LAL, Université Paris-Sud, CNRS/IN2P3, Orsay, France*
[8] *LPNHE, Université Pierre et Marie Curie, Université Paris Diderot, CNRS/IN2P3, Paris, France*
[9] *Fakultät Physik, Technische Universität Dortmund, Dortmund, Germany*
[10] *Max-Planck-Institut für Kernphysik (MPIK), Heidelberg, Germany*
[11] *Physikalisches Institut, Ruprecht-Karls-Universität Heidelberg, Heidelberg, Germany*
[12] *School of Physics, University College Dublin, Dublin, Ireland*
[13] *Sezione INFN di Bari, Bari, Italy*
[14] *Sezione INFN di Bologna, Bologna, Italy*
[15] *Sezione INFN di Cagliari, Cagliari, Italy*
[16] *Sezione INFN di Ferrara, Ferrara, Italy*
[17] *Sezione INFN di Firenze, Firenze, Italy*

[18] Laboratori Nazionali dell'INFN di Frascati, Frascati, Italy
[19] Sezione INFN di Genova, Genova, Italy
[20] Sezione INFN di Milano Bicocca, Milano, Italy
[21] Sezione INFN di Roma Tor Vergata, Roma, Italy
[22] Sezione INFN di Roma La Sapienza, Roma, Italy
[23] Nikhef National Institute for Subatomic Physics, Amsterdam, Netherlands
[24] Nikhef National Institute for Subatomic Physics and Vrije Universiteit, Amsterdam, Netherlands
[25] Henryk Niewodniczanski Institute of Nuclear Physics Polish Academy of Sciences, Cracow, Poland
[26] Faculty of Physics & Applied Computer Science, Cracow, Poland
[27] Soltan Institute for Nuclear Studies, Warsaw, Poland
[28] Horia Hulubei National Institute of Physics and Nuclear Engineering, Bucharest-Magurele, Romania
[29] Petersburg Nuclear Physics Institute (PNPI), Gatchina, Russia
[30] Institute of Theoretical and Experimental Physics (ITEP), Moscow, Russia
[31] Institute of Nuclear Physics, Moscow State University (SINP MSU), Moscow, Russia
[32] Institute for Nuclear Research of the Russian Academy of Sciences (INR RAN), Moscow, Russia
[33] Budker Institute of Nuclear Physics (SB RAS) and Novosibirsk State University, Novosibirsk, Russia
[34] Institute for High Energy Physics (IHEP), Protvino, Russia
[35] Universitat de Barcelona, Barcelona, Spain
[36] Universidad de Santiago de Compostela, Santiago de Compostela, Spain
[37] European Organization for Nuclear Research (CERN), Geneva, Switzerland
[38] Ecole Polytechnique Fédérale de Lausanne (EPFL), Lausanne, Switzerland
[39] Physik-Institut, Universität Zürich, Zürich, Switzerland
[40] NSC Kharkiv Institute of Physics and Technology (NSC KIPT), Kharkiv, Ukraine
[41] Institute for Nuclear Research of the National Academy of Sciences (KINR), Kyiv, Ukraine
[42] H.H. Wills Physics Laboratory, University of Bristol, Bristol, United Kingdom
[43] Cavendish Laboratory, University of Cambridge, Cambridge, United Kingdom
[44] Department of Physics, University of Warwick, Coventry, United Kingdom
[45] STFC Rutherford Appleton Laboratory, Didcot, United Kingdom
[46] School of Physics and Astronomy, University of Edinburgh, Edinburgh, United Kingdom
[47] School of Physics and Astronomy, University of Glasgow, Glasgow, United Kingdom
[48] Oliver Lodge Laboratory, University of Liverpool, Liverpool, United Kingdom
[49] Imperial College London, London, United Kingdom
[50] School of Physics and Astronomy, University of Manchester, Manchester, United Kingdom
[51] Department of Physics, University of Oxford, Oxford, United Kingdom
[52] Syracuse University, Syracuse, NY, United States
[53] CC-IN2P3, CNRS/IN2P3, Lyon-Villeurbanne, France, associated member
[54] Pontifícia Universidade Católica do Rio de Janeiro (PUC-Rio), Rio de Janeiro, Brazil, associated to [2]

[a] P.N. Lebedev Physical Institute, Russian Academy of Science (LPI RAS), Moscow, Russia
[b] Università di Bari, Bari, Italy
[c] Università di Bologna, Bologna, Italy
[d] Università di Cagliari, Cagliari, Italy
[e] Università di Ferrara, Ferrara, Italy
[f] Università di Firenze, Firenze, Italy
[g] Università di Urbino, Urbino, Italy
[h] Università di Modena e Reggio Emilia, Modena, Italy
[i] Università di Genova, Genova, Italy
[j] Università di Milano Bicocca, Milano, Italy
[k] Università di Roma Tor Vergata, Roma, Italy
[l] Università di Roma La Sapienza, Roma, Italy
[m] Università della Basilicata, Potenza, Italy
[n] LIFAELS, La Salle, Universitat Ramon Llull, Barcelona, Spain
[o] Institució Catalana de Recerca i Estudis Avançats (ICREA), Barcelona, Spain
[p] Hanoi University of Science, Hanoi, Viet Nam

A search is performed for the lepton number violating decay $B^+ \to h^- \mu^+ \mu^+$, where h^- represents a K^- or a π^-, using data from the LHCb detector corresponding to an integrated luminosity of $36\,\mathrm{pb}^{-1}$. The decay is forbidden in the Standard Model but allowed in models with a Majorana neutrino. No signal is observed in either channel and limits of $\mathcal{B}(B^+ \to K^- \mu^+ \mu^+) < 5.4 \times 10^{-8}$ and $\mathcal{B}(B^+ \to \pi^- \mu^+ \mu^+) < 5.8 \times 10^{-8}$ are set at the 95% confidence level. These improve the previous best limits by factors of 40 and 30, respectively.

PACS numbers: 11.30.Fs, 13.20.He, 13.35.Hb

Lepton number is conserved in the Standard Model but can be violated in a range of new physics models such as those with Majorana neutrinos [1] or left-right symmetric models with a doubly charged Higgs boson [2]. In this

letter a search for lepton number violating decays of the type $B^+ \to h^-\mu^+\mu^+$, where h^- represents a K^- or a π^-, is presented. The inclusion of charge conjugated modes is implied throughout. A search for any lepton number violating process that mediates the $B^+ \to h^-\mu^+\mu^+$ decay is made. A specific search for $B^+ \to h^-\mu^+\mu^+$ decays mediated by an on-shell Majorana neutrino (Fig. 1) is also performed. Such decays would give rise to a narrow peak in the invariant mass spectrum of the hadron and one of the muons [3], $m_\nu = m_{h\mu}$, if the mass of the neutrino is between $m_{K(\pi)}+m_\mu$ and m_B-m_μ. The previous best experimental limit on the $B^+ \to K^-(\pi^-)\mu^+\mu^+$ branching fraction is $1.8(1.2) \times 10^{-6}$ at 90% confidence level (CL) [4].

The search for $B^+ \to h^-\mu^+\mu^+$ is carried out with data from the LHCb experiment at the Large Hadron Collider at CERN. The data corresponds to $36\,\text{pb}^{-1}$ of integrated luminosity of proton-proton collisions at $\sqrt{s} = 7\,\text{TeV}$ collected in 2010. The LHCb detector is a single-arm spectrometer designed to study b-hadron decays with an acceptance for charged tracks with pseudorapidity between 2 and 5. Primary proton-proton vertices (PVs), and secondary B vertices are identified in a silicon strip vertex detector. Tracks from charged particles are reconstructed by the vertex detector and a set of tracking stations. The curvature of the tracks in a dipole magnetic field allows momenta to be determined with a precision of $\delta p/p = 0.35$–0.5%. Two Ring Imaging CHerenkov (RICH) detectors allow kaons to be separated from pions/muons over a momentum range $2 < p < 100\,\text{GeV}/c$. Muons with momentum above $3\,\text{GeV}/c$ are identified on the basis of the number of hits left in detectors interleaved with an iron muon filter. Further details about the LHCb detector can be found in Ref. [5].

The search for $B^+ \to h^-\mu^+\mu^+$ decays is based on the selection of $B^+ \to h^\pm\mu^+\mu^\mp$ candidates. The $B^+ \to J/\psi K^+$ decay with $J/\psi \to \mu^+\mu^-$ is included in the same selection. It is subsequently used as a normalisation mode when setting a limit on the branching fraction of the $B^+ \to h^-\mu^+\mu^+$ decays. The selection is designed to minimise and control the difference between decays with same- and opposite-sign muons and thus cancel most of the systematic uncertainty from the normalisation. The only differences in efficiency between the signal and normalisation channels are due to the decay kinematics and the presence of a same-sign muon pair, rather than an opposite-sign pair, in the final state.

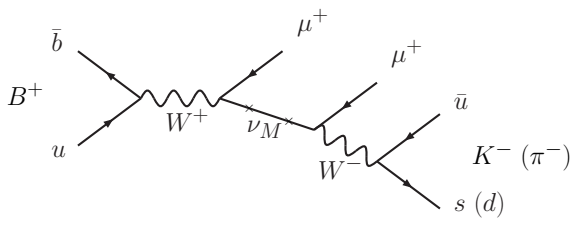

FIG. 1. s-channel diagram for $B^+ \to K^-\mu^+\mu^+$ ($B^+ \to \pi^-\mu^+\mu^+$) where the decay is mediated by an on-shell Majorana neutrino.

In the trigger, the $B^+ \to h^\pm\mu^+\mu^\mp$ candidates are required to pass the initial hardware trigger based on the p_T of one of the muons. In the subsequent software trigger, one of the muons is required to have a large impact parameter (IP) with respect to all the PVs in the event and to pass requirements on the quality of the track fit and the compatibility of the candidate with the muon hypothesis. Finally, the muon candidate combined with another track is required to form a vertex displaced from the PVs.

Further event selection is applied offline on fully reconstructed B decay candidates. The selection is designed to reduce combinatorial backgrounds, where not all the selected tracks come from the same decay vertex; and peaking backgrounds, where a single decay is selected but with some of the particle types misidentified. The combinatorial background is smoothly distributed in the reconstructed B-candidate mass and the level of background is assessed from the sidebands around the signal window. Peaking backgrounds from B decays to hadronic final states, final states with a J/ψ and semileptonic final states are also considered.

Proxies are used in the optimisation of the selection for both the signal and the background to avoid a selection bias. The $B^+ \to J/\psi K^+$ decay is used as a proxy for the signal. The background proxy comprises opposite-sign $B^+ \to h^+\mu^+\mu^-$ candidates with an invariant mass in the upper mass sideband and with muon pairs incompatible with a J/ψ or a $\psi(2S)$ hypothesis. The bias introduced by using $B^+ \to J/\psi K^+$ for both optimisation and as a normalisation mode is insignificant due to the large number of candidates.

The combinatorial background is reduced by requiring that the decay products of the B have $p_\text{T} > 800\,\text{MeV}/c$. Tracks are selected which are incompatible with originating from a PV based on the χ^2 of the tracks' impact parameters ($\chi^2_\text{IP} > 45$). The direction of the candidate B^+ momentum is required to be within 8 mrad of the reconstructed B^+ line of flight. The B^+ vertex is also required to be of good quality ($\chi^2 < 12$ for three degrees of freedom) and significantly displaced from the PV (χ^2 of vertex separation larger than 144).

The selection uses a range of particle identification (PID) criteria, based on information from the RICH and muon detectors, to ensure the hadron and the muons are correctly identified. For example, $\text{DLL}_{K\pi}$ is the difference in log-likelihoods between the K and π hypotheses. For the $B^+ \to K^-\mu^+\mu^+$ final state, $\text{DLL}_{K\pi} > 1$ is required to select kaon candidates. For the $B^+ \to \pi^-\mu^+\mu^+$ final state the selection criterion is mirrored to select pions with $\text{DLL}_{K\pi} < -1$. The $B^+ \to K^-\mu^+\mu^+$ and

$B^+ \to \pi^-\mu^+\mu^+$ selections are otherwise identical.

To reject background events where two tracks that are close together in the tracking system share hits in the muon detector, a requirement is made on the maximum number of muon system hits that two candidate muons may have in common. This requirement can introduce a bias in the relative efficiency between signal and normalisation channels, as both tracks from the same-sign muon pair for $B^+ \to h^-\mu^+\mu^+$ will curve in the same direction in the dipole field. Simulated events give an estimate of 0.3% for the effect on the relative efficiency between the signal and normalisation channel. In order to avoid selecting a muon as the pion or kaon, the candidate hadron is also required to be within the acceptance of the muon system but not have a track segment there.

After the application of the above criteria the combinatorial background is completely dominated by candidates with two real muons, rather than by hadrons misidentified as muons.

The invariant mass distribution and the relevant misidentification rates are required in order to evaluate the peaking background. These are evaluated, respectively, from a full simulation using PYTHIA [6] followed by GEANT4 [7], and from control channels which provide an unambiguous and pure source of particles of known type. The control channel events are selected to have the same kinematics as the signal decay, without the application of any PID criteria. $D^* \to D^0\pi$, $D^0 \to K\pi$ decays give pure sources of pions and kaons. A pure source of muons is selected by using a *tag-and-probe* approach with $J/\psi \to \mu^+\mu^-$ decays [8].

Under the $B^+ \to K^-\mu^+\mu^+$ hypothesis, any crossfeed from $B^+ \to J/\psi K^+$ decays would peak strongly in the signal mass region. The $K \to \mu$ mis-id rate is evaluated from the above D^* sample and the $\mu \to K$ mis-id rate from the J/ψ sample. The later mis-id rate is consistent with zero. The number of $B^+ \to J/\psi K^+$ events expected in the signal region is therefore also zero but with a large uncertainty which dominates the error on the total exclusive background expected in the signal region. The $B^+ \to \pi^-\pi^+K^+$ decay contributes the most to the peaking background with an expected $(1.7 \pm 0.1) \times 10^{-3}$ candidates, followed by the $B^+ \to K^-\pi^+K^+$ decay with $(6.1 \pm 0.8) \times 10^{-4}$ candidates. The total peaking background expected in the $B^+ \to K^-\mu^+\mu^+$ signal region is $(3.4^{+14.0}_{-0.2}) \times 10^{-3}$ events with the asymmetric error caused by the zero expectation from the $B^+ \to J/\psi K^+$ decay.

Under the $B^+ \to \pi^-\mu^+\mu^+$ hypothesis, $B^+ \to J/\psi K^+$ decays are reconstructed with invariant masses below the nominal B^+ mass, in the lower mass sideband. The dominant background decay in this case is $B^+ \to \pi^-\pi^+\pi^+$, where the two same-sign pions are misidentified as muons. The $B^+ \to \pi^-\mu^+\mu^+$ peaking background level is $(2.9 \pm 0.6) \times 10^{-2}$ events.

In Fig. 2(a), the $m_{K^+\mu^+\mu^-}$ invariant mass distribution for $B^+ \to K^+\mu^+\mu^-$ events with $|m_{\mu^+\mu^-} - m_{J/\psi}| < 50\,\text{MeV}/c^2$ is shown, after the application of the selection. In the $B^+ \to J/\psi K^+$ sample, there are no events containing more than one candidate. An unbinned maximum likelihood fit to the $B^+ \to J/\psi K^+$ mass peak is made with a Crystal Ball [9] function which accounts for the radiative tail. The combinatorial background is assumed to be flat, and the partially reconstructed events in the lower mass sideband are fitted with a Gaussian distribution. The signal peak has a Gaussian component of width $20\,\text{MeV}/c^2$, and a signal mass window of $5280 \pm 40\,\text{MeV}/c^2$ is chosen. The $B^+ \to J/\psi K^+$ peak contains 3407 ± 59 signal events within the signal window. $B^+ \to J/\psi \pi^+$ candidates were also examined and, accounting for a shoulder in the mass distribution from $B^+ \to J/\psi K^+$, the yield observed agrees with the expectation.

The $m_{K^+\mu^+\mu^-}$ invariant mass distribution for events with $|m_{\mu^+\mu^-} - m_{J/\psi,\psi(2S)}| > 70\,\text{MeV}/c^2$ is shown in Fig. 2(b). Using the same fit model, with all shape parameters fixed to those from the above fit, the signal peak was determined to contain 27 ± 5 events from the $B^+ \to K^+\mu^+\mu^-$ decay. The ratio of branching fractions between $B^+ \to J/\psi K^+$ and $B^+ \to K^+\mu^+\mu^-$ decays [10] and the trigger efficiency ratio predicted by the simu-

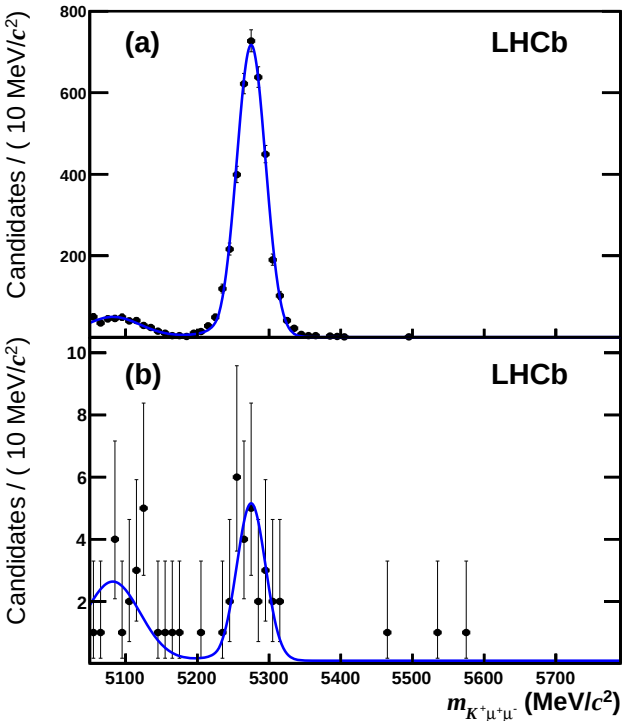

FIG. 2. Invariant mass distribution of $K^+\mu^+\mu^-$ events after the application of the selection criteria. In (a) requiring the muon pair to be compatible with coming from a J/ψ decay and in (b) excluding invariant mass windows around the J/ψ and $\psi(2S)$ for the muon pair. The curve is the fit to data as described in the text.

lation, give an expectation of 29 ± 4 $B^+ \to K^+\mu^+\mu^-$ decays. The observed yield is consistent with the expectation showing that the selection does not favour candidates with a dimuon mass close to the J/ψ mass.

The difference in efficiency between the signal and normalisation channels was evaluated using Monte Carlo simulation samples. The relative selection efficiency across the phase space is shown for $B^+ \to K^-\mu^+\mu^+$ in Fig. 3. The efficiency of the signal selection in a given phase space bin is divided by the average efficiency of $B^+ \to J/\psi K^+$, to yield the relative efficiency for that bin. The D^* control channel is used to determine the PID efficiencies required to normalise $B^+ \to \pi^-\mu^+\mu^+$ to $B^+ \to J/\psi K^+$.

Assuming a signal that is uniformly distributed in phase space, the relative efficiency of $B^+ \to K^-\mu^+\mu^+$ and $B^+ \to J/\psi K^+$ was calculated to be $89.1 \pm 0.4\,(\text{stat}) \pm 0.3\,(\text{syst})\%$. The relative efficiency of $B^+ \to \pi^-\mu^+\mu^+$ and $B^+ \to J/\psi K^+$ was calculated to be $82.7 \pm 0.6\,(\text{stat}) \pm 0.8\,(\text{syst})\%$. The systematic uncertainties associated with these estimates are detailed below. These relative efficiencies together with the number of events observed in the normalisation channel, give single event sensitivities of 2.0×10^{-8} (2.1×10^{-8}) in the $B^+ \to K^-\mu^+\mu^+$ ($B^+ \to \pi^-\mu^+\mu^+$) case.

In order to compute the efficiency under a given Majorana neutrino mass hypothesis, a model for the variation of efficiency with $m_{h\mu}$ is required. For a given value of $m_{h\mu}$ this is obtained by varying the polarisation of the Majorana neutrino in the decay and taking the lowest (most conservative) value of the efficiency.

The dominant systematic uncertainty (under the assumption of a flat phase-space distribution) for the single event sensitivity is the 3.4% uncertainty on the $B^+ \to J/\psi K^+$ branching fraction. The statistical uncertainty

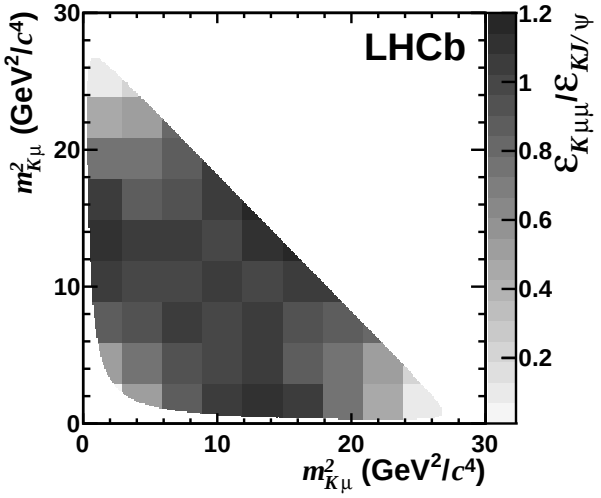

FIG. 3. Relative efficiency between the $B^+ \to K^-\mu^+\mu^+$ signal and the $B^+ \to J/\psi K^+$ normalisation channel. The plot has been symmetrised over the diagonal.

TABLE I. Sources of systematic error and their fractional uncertainty on the relative efficiency.

Source	$B^+ \to K^-\mu^+\mu^+$	$B^+ \to \pi^-\mu^+\mu^+$
$\mathcal{B}(B^+ \to J/\psi K^+)$	3.4%	3.4%
$B^+ \to J/\psi K^+$ yield	1.7%	1.7%
$B^+ \to J/\psi K^+$ fit models	1.6%	1.6%
Simulation statistics	0.4%	0.6%
IP modelling	0.2%	0.2%
PID modelling	0.1%	0.8%
Trigger efficiency	0.1%	0.1%
Tracking efficiency	0.1%	0.1%

on the $B^+ \to J/\psi K^+$ yield gives an additional systematic uncertainty of 1.7% and the uncertainty from the model used to fit the data is 1.6%. The latter is evaluated by changing the Crystal Ball signal function used in the fit to a Gaussian and the polynomial background function to an exponential.

There are several sources of uncertainty associated with the calculation of the relative efficiency between the signal and normalisation channels. In addition to the statistical uncertainty of the simulation samples, there are systematic uncertainties from: the differences in the effect of the IP selection criteria between the simulation and data; the statistical uncertainty on the measured PID efficiencies; the uncertainties associated with the simulation of the trigger; and the uncertainty in the tracking efficiency. In each case the systematic uncertainty is estimated by varying the relevant criteria at the level of the expected effect and re-evaluating the relative efficiency. For the $B^+ \to \pi^-\mu^+\mu^+$ decay, there is an additional uncertainty from the correction for the relative kaon- and pion-identification efficiencies. The systematic uncertainties averaged over the three-body phase space are given in Table I.

A limit on the branching fraction of each of the $B^+ \to h^-\mu^+\mu^+$ decays is set by counting the number of observed events in the mass windows, and using the single event sensitivity. The probability is modelled with a Poisson distribution where the mean has contributions from a potential signal, the combinatorial and peaking backgrounds. The combinatorial background is unconstrained by measurements from the simulation or the opposite-sign data. The number of events in the upper mass sideband is therefore used to constrain the contribution of the combinatorial background to the Poisson mean. The upper mass sideband is restricted to masses above $m_{h\mu\mu} > 5.4\,\text{GeV}/c^2$ such that any peaking background component can be ignored. In both the $B^+ \to K^-\mu^+\mu^+$ and $B^+ \to \pi^-\mu^+\mu^+$ cases no events are found in either the upper or lower mass sidebands. This is consistent with the observation of three opposite-sign candidates seen in the $B^+ \to K^+\mu^+\mu^-$ upper mass side-

band (Fig. 2) and two candidates in the $B^+ \to \pi^+\mu^+\mu^-$ upper mass sideband. The peaking background estimates are explicitly split into two components, the contribution from $B^+ \to h^-h^+h^+$ decays and that from $B^+ \to J/\psi\, K^+$ decays. The latter has a large uncertainty. The central values for both peaking background components are taken from the estimates described above.

Systematic uncertainties on the peaking background, single event sensitivity and signal-to-sideband scale factor are included in the limit-setting procedure using a Bayesian approach. The unknown parameter is integrated over and included in the probability to observe a given number of events in the signal and upper mass window.

In the signal mass windows of $B^+ \to K^-\mu^+\mu^+$ and $B^+ \to \pi^-\mu^+\mu^+$ no events are observed. This corresponds to limits on the $B^+ \to h^-\mu^+\mu^+$ branching fractions of

$$\mathcal{B}(B^+ \to K^-\mu^+\mu^+) < 5.4\,(4.1) \times 10^{-8} \text{ at } 95\%\,(90\%) \text{ CL},$$
$$\mathcal{B}(B^+ \to \pi^-\mu^+\mu^+) < 5.8\,(4.4) \times 10^{-8} \text{ at } 95\%\,(90\%) \text{ CL}.$$

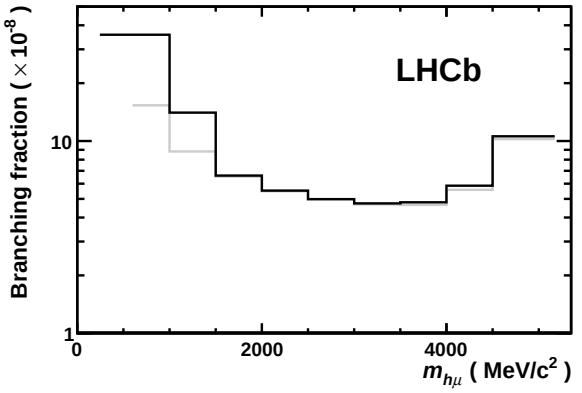

FIG. 4. The 95 % CL branching fraction limits for $B^+ \to K^-\mu^+\mu^+$ (light-coloured line) and $B^+ \to \pi^-\mu^+\mu^+$ (dark-coloured line) as a function of the Majorana neutrino mass $m_\nu = m_{h\mu}$.

The observation of no candidates in the sidebands as well as the signal region is compatible with a background-only hypothesis. The $m_{h\mu}$ dependence of the limit in models where the Majorana neutrino can be produced on mass shell is shown in Fig. 4. The shapes of the limits arise from the changing efficiency as a function of mass.

In summary, a search for the $B^+ \to K^-\mu^+\mu^+$ and $B^+ \to \pi^-\mu^+\mu^+$ decays modes has been performed with $36\,\text{pb}^{-1}$ of integrated luminosity collected with the LHCb detector in 2010. No signal is observed in either decay and, using $B^+ \to J/\psi\, K^+$ as a normalisation channel, the present best limits on $\mathcal{B}(B^+ \to K^-\mu^+\mu^+)$ and $\mathcal{B}(B^+ \to \pi^-\mu^+\mu^+)$ are improved by factors of 40 and 30, respectively [4].

ACKNOWLEDGMENTS

We express our gratitude to our colleagues in the CERN accelerator departments for the excellent performance of the LHC. We thank the technical and administrative staff at CERN and at the LHCb institutes, and acknowledge support from the National Agencies: CAPES, CNPq, FAPERJ and FINEP (Brazil); CERN; NSFC (China); CNRS/IN2P3 (France); BMBF, DFG, HGF and MPG (Germany); SFI (Ireland); INFN (Italy); FOM and NWO (Netherlands); SCSR (Poland); ANCS (Romania); MinES of Russia and Rosatom (Russia); MICINN, XuntaGal and GENCAT (Spain); SNSF and SER (Switzerland); NAS Ukraine (Ukraine); STFC (United Kingdom); NSF (USA). We also acknowledge the support received from the ERC under FP7 and the Région Auvergne.

[1] E. Majorana, *Teoria simmetrica dell'elettrone e del positrone*, *Nuovo Cim.* **14** (1937) 171–184.

[2] J. C. Pati and A. Salam, *Lepton Number as the Fourth Color*, *Phys. Rev.* **D10** (1974) 275–289. Erratum-ibid. **D11** (1975) 703.

[3] S. Pascoli and S. Petcov, *Majorana Neutrinos, Neutrino Mass Spectrum and the $|\langle m\rangle| \sim 10^{-3}$ eV Frontier in Neutrinoless Double Beta Decay*, *Phys. Rev.* **D77** (2008) 113003, [arXiv:0711.4993].

[4] CLEO collaboration, K. W. Edwards et al., *Search for lepton flavor violating decays of B mesons*, *Phys. Rev.* **D65** (2002) 111102, [arXiv:hep-ex/0204017].

[5] LHCb collaboration, A. A. Alves et al., *The LHCb Detector at the LHC*, *JINST* **3** (2008) S08005.

[6] T. Sjöstrand, S. Mrenna, and P. Z. Skands, *PYTHIA 6.4 Physics and Manual*, *JHEP* **05** (2006) 026, [arXiv:hep-ph/0603175].

[7] GEANT4 collaboration, S. Agostinelli et al., *GEANT4: A simulation toolkit*, *Nucl. Instrum. Meth.* **A506** (2003) 250–303.

[8] LHCb collaboration, R. Aaij et al., *Search for the rare decays $B_s^0 \to \mu^+\mu^-$ and $B^0 \to \mu^+\mu^-$*, *Phys. Lett.* **B699** (2011) 330–340, [arXiv:1103.2465].

[9] T. Skwarnicki, *A study of the radiative cascade transitions between the Upsilon-prime and Upsilon resonances*. PhD thesis, Institute of Nuclear Physics, Krakow, 1986. DESY-F31-86-02.

[10] Particle Data Group, K. Nakamura et al., *Review of particle physics*, *J. Phys.* **G37** (2010) 075021.